



Spatiotemporal variability of the ocean since 1900: testing a new analysis approach using global sea level reconstruction

Tal Ezer¹ · Sönke Dangendorf¹

Received: 12 July 2021 / Accepted: 8 December 2021 / Published online: 29 December 2021
© Springer-Verlag GmbH Germany, part of Springer Nature 2021

Abstract

A new approach for analysis of spatiotemporal variability across ocean basins was tested using global $1^\circ \times 1^\circ$ monthly sea level reconstruction (RecSL) for 1900–2015. Each sea level cross section $\eta(x,t)$ was converted into a single time series that contains both spatial and temporal variabilities by connecting back and forth repeated monthly sections. For example, a single zonal section between 50°W and 50°E would create a time series of $116 \text{ years} \times 12 \text{ months} \times 100^\circ = 139,200$ data points. The long record allowed great statistical significance and direct comparison between energy in spatial variability and energy in temporal variability. Time and length scales found in 116 years of RecSL data are compared with 23 years of altimeter data. Empirical Mode Decomposition (EMD) was then used to break the record into high-frequency modes representing spatial variability across the section and lower frequency modes representing temporal variability (capturing time scales of a few months to multidecadal). Examples of the spatiotemporal analysis in the Pacific Ocean showed how the method detected an increase in El Niño amplitude in equatorial regions and characterized spatiotemporal changes in the Kuroshio Current in mid-latitudes. In the Atlantic Ocean, the analysis showed the latitudinal dependency of spatiotemporal variability: for example, sections near the Gulf Stream (GS) and the Antarctic Circumpolar Current (ACC) showed energy dominated by small-scale spatial variability while sections across equatorial and subpolar North Atlantic regions showed energy dominated by long-term temporal variability and diminishing energy in spatial variability. The impact of the North Atlantic Oscillation (NAO) index on spatiotemporal variability showed that interannual variations in NAO are highly correlated with subpolar sea level variability, while decadal and longer variations in NAO are linked with sea level variations at the equatorial South Atlantic and the Antarctic zone. This analysis can be useful for other observations and various climate data.

Keywords Spatiotemporal variability · Sea level · Climate change

1 Introduction

Studies of sea level rise (SLR) and sea level variability (Church and White 2006, 2011; Merrifield et al. 2009; Jevrejeva et al. 2008; Hay et al. 2015; Dangendorf et al. 2014, 2017, 2019; Ezer and Dangendorf 2020, 2021) often show considerable nonhomogeneity; for example, some locations

have larger SLR acceleration than others, and regions near western boundary currents have a lot more mesoscale variability than, for instance, centers of subtropical gyres. Different regions are also subject to different forcing that operate on different time scales and these forcing may change over time due to climate change. For example, changes in water masses (barystatic sea level change) due to land-ice melting and hydrological processes may be more dominant in the future than contribution to SLR from changes in steric sea level due to changes in salinity and temperature, particularly at multidecadal scales (Frederikse et al. 2020). Moreover, both barystatic and steric sea level changes have strong spatial and mostly latitudinal variations (Ezer and Dangendorf 2021), so spatiotemporal changes need to be considered. Climatic shifts in one location can influence other regions—for example, shifts in Southern Ocean winds (Cai 2006) were linked with sea level acceleration in northern latitudes after

Responsible Editor: Tal Ezer

Revision Submitted to *Ocean Dynamics* on October 06, 2021, final version: December 07, 2021

✉ Tal Ezer
tezer@odu.edu

¹ Center for Coastal Physical Oceanography, Old Dominion University, 4111 Monarch Way, Norfolk, VA 23508, USA

the 1960s (Dangendorf et al. 2019). Latitudinal variations in spatiotemporal variability are also related to the combined impact of Earth's rotation, i.e., the Coriolis effect, and stratification, so for example, the baroclinic Rossby radius of deformation that determines spatial scales in the ocean is largely geographically dependent (Chelton et al. 1998). Turbulence spectrum of oceanic flows can also be latitudinal-dependent since mesoscale and sub-mesoscale variability can be affected by Coriolis, as recently shown by Galperin et al. (2021).

Therefore, one of the goals of this study is to see how spatiotemporal variations change with latitude. Some studies suggest also that climate change may intensify or shift the path of western boundary currents (WBCs) and increase eddy activities there (Wu et al. 2012; Beal and Elipot 2016; Yang et al. 2016; Han et al. 2019; Chen et al. 2019; Ezer and Dangendorf 2020, 2021; Martínez-Moreno et al. 2021; Sen Gupta et al. 2021). These WBCs contain much of the kinetic energy of the upper ocean and the mesoscale variability, so an important question is how variations over time will affect spatial variability. Although our analysis does not directly resolve mesoscale and sub-mesoscale eddies, these eddies contribute to the general kinetic energy of the ocean and play an important role in the heat and salt transports (Dong et al. 2014), so it is crucial to understand the spatiotemporal ocean variability and potential changes over time. In the Atlantic Ocean, the dominant current is the Gulf Stream, which is closely linked with variations in the North Atlantic Oscillation, NAO, and the Atlantic Meridional Overturning Circulation, AMOC (Bryden et al. 2005; McCarthy et al. 2012; Sallenger et al. 2012; Blaker et al. 2014; Ezer et al. 2013; Ezer 2015; Rahmstorf et al. 2015; Caesar et al. 2018; Smeed et al. 2018; Little et al. 2019; Zhang et al. 2020). An important question is how does potential future weakening of AMOC and other time-dependent changes may affect the Gulf Stream spatial variability? Even within the Gulf Stream itself, long-term trends can be very different when comparing sections separated by only 2° (Andres et al. 2020), so better understanding of the spatiotemporal variability and its sources is needed. The goal here is to demonstrate a new method to analyze the combined variability in space and time to provide a tool to study spatiotemporal variability in the ocean. Unlike more common spatiotemporal methods such as Empirical Orthogonal Function (EOF) analysis that are widely used to study ocean variability (e.g., Oey et al. 2004) and separates data into spatial modes and time-dependent time series, the method tested here treats time and space variabilities the same way, which allows direct comparison between spatial and temporal variability, as described below.

There are different ways to study spatiotemporal variability. Mann and Park (1996), for example, used multivariate frequency domain singular value decomposition (SVD) to

study spatiotemporal modes of climatic variability in sea level pressure and surface temperature. They looked at oscillating interannual and climate modes, their forcing, and their geographical distribution. The analysis also allowed studying how frequency and amplitude of climate modes evolve in time—this trait of the analysis is similar to that of the Empirical Mode Decomposition (EMD) analysis used here. Another example is the study of Serazin et al. (2015), who used high-resolution model-derived global sea level and decomposed the data into few frequency-wavenumber bins, looking at spatial variability at “small-scale” of less than 6° versus “large-scale” of more than 12° and looking at two temporal time scales of “high-frequency” and “low-frequency,” separated by the 18-month period. They found that most of the small-scale variability is intrinsic oceanic in origin with little atmospheric influence, while large-scale low-frequency variability is largely driven by atmospheric variability. They used Lanczos temporal and spatial filters to separate the different scales. Our approach, as described in the next section, is somewhat different and more general in the sense that it tries to analyze the full continuous spectrum of spatial and temporal scales without artificially selecting particular cutoffs. The identification of different spatial and temporal scales and their energy is done using the nonstationary, nonparametric EMD approach (Huang et al. 1998; Wu and Huang 2004; Wu et al. 2007; Wu and Huang 2009; Ezer et al. 2013; Ezer 2015). Note, however, that the sea level reconstruction (RecSL) that was used to test the method (Dangendorf et al. 2019) has 1° spatial resolution and monthly temporal resolution, putting limits on the smallest spatial scales and highest frequency that can be resolved. On the other hand, RecSL covers 116 years, so long-term decadal and multidecadal variability can be detected; a comparison with 23 years of altimeter data will provide further assessment of the method and the reconstruction.

The two main goals of this study are as follows: first, to introduce and test a new spatiotemporal analysis method, and second, to demonstrate its usefulness in studies of sea level variability, potential forcing mechanisms, and the latitudinal variations. The paper is organized as follows: the data and the analysis methods are described in Sect. 2; then in Sect. 3, the results are described, first for sections across the Pacific Ocean, and then for the Atlantic Ocean with a discussion of links to the North Atlantic Oscillations. Finally, in Sect. 4, a summary and conclusions are offered.

2 Data sources and analysis methods

To demonstrate and test the new analysis method, we used the monthly global reconstructed sea level (RecSL) on a ($1^\circ \times 1^\circ$) grid for 1900–2015 (Dangendorf et al. 2019); this data set was recently used in several studies (Dangendorf

et al. 2021; Ezer and Dangendorf 2020, 2021; Frederikse et al. 2020; Gehrels et al. 2020). This hybrid reconstruction is based on a combination of tide gauge records, satellite altimeter data, and several geophysical ancillary datasets (for details of reconstruction methods and global sea level components, see the references above, as well as Hay et al. 2015, Calafat et al. 2014 and Gregory et al. 2019). The seasonal cycle was removed from the RecSL record, but sea level rise trend remains. Altimeter data (available from the Copernicus Marine service <https://marine.copernicus.eu/>) were interpolated into the RecSL grid and used to see how spatiotemporal variability in the shorter altimeter record (1993–2015) is compared with the much longer RecSL record (1900–2015), which rely mostly on tide gauge data for earlier years.

Various analysis methods can be used to analyze and present spatiotemporal variability, from simple Hovmöller diagrams to statistically based methods such as wavelet analysis (e.g., Grinsted et al. 2004), singular value decomposition, SVD (e.g., Mann and Park 1996), EOF analysis (e.g., Oey et al. 2004), or EMD (Ezer et al. 2013; Ezer 2015). However, most methods usually treat spatial and temporal variations separately or use space–time filters. Analysis of spatiotemporal sea level variability by Serazin et al. (2015), for example, separated spatial variability and temporal variability into chosen small-scale high-frequency and large-scale low-frequency windows. It should be emphasized that many oceanic processes such as Rossby waves contribute to both spatial and temporal variabilities, so separating spatial and temporal variabilities does not necessarily mean separating different processes. In contrast to most other methods mentioned above, here the spatial and temporal variations at each latitude were composed into a single time series, allowing a direct comparison of energy in spatial scales and temporal scales. To the best of our knowledge, the new analysis method described here has not been used this way before. The method is demonstrated here using sea level variability in zonal cross sections $\eta(x, Y, t)$, where Y is a chosen latitude, $X_1 < x < X_2$ ($\Delta x = 1^\circ$) is a longitude range, and $1900 < t < 2015$ ($\Delta t = 1$ month interval) is time. The analysis comprises of the following steps:

Step I: The two-dimensional (in space and time) sea level section $\eta(x, Y, t)$, is converted into a one-dimensional time series that contains both spatial and temporal variabilities by connecting back and forth repeated monthly sections (the change in direction eliminates discontinuity at the edges) so that for a section along Y ,

$$\begin{aligned}
 \eta(t_1) &= [\eta(X_1, t_1), \eta(X_1, \Delta x, t_1), \eta(X_1, 2\Delta x, t_1) \dots, \eta(X_2, t_1)] \text{ (Jan.1990)} \\
 \eta(t_2) &= [\eta(X_2, t_2), \eta(X_2, \Delta x, t_2), \eta(X_2, 2\Delta x, t_2) \dots, \eta(X_1, t_2)] \text{ (Feb.1990)} \\
 &\dots \\
 \eta(t_N) &= [\eta(X_1, t_N), \eta(X_1, \Delta x, t_N), \eta(X_1, 2\Delta x, t_N) \dots, \eta(X_2, t_N)] \text{ (Dec, 2015)} \\
 \text{final time series} &: \eta(t) = [\eta(t_1), \eta(t_2), \dots, \eta(t_N)]
 \end{aligned} \tag{1}$$

For example, a section from $X_1 = 50^\circ\text{W}$ to $X_2 = 50^\circ\text{E}$ would have a time series of $116 \text{ years} \times 12 \text{ months} \times 100^\circ = 139,200$ data points. The long record allowed analysis with a greater statistical significance than analyzing spatial or temporal variations separately. For temporal variability in this example, there are 100 times more data points than say analyzing the mean sea level of that section, and for spatial variability, there are $116 \times 12 = 1392$ times more data points than any single cross section. The method of connecting data by a “back-and-forth” method eliminates discontinuity near the boundaries. Nevertheless, variations in grid points near boundaries and variability near monthly cycles are still less reliable, so only temporal variations with periods of at least a few months are discussed.

Step II: Remove the time-mean at each point to get an anomaly time series $\eta'(t)$. This will remove for example a sea level difference between the eastern and western side of ocean basins or a sea level slope across western boundary currents, but local variability and sea level rise will remain. Plots, shown later, will demonstrate the data before and after this step, with the former (in step I) showing changes for example in spatial sea level gradients across WBCs, while the latter (in step II) showing for example variations in time at a particular location in a section. Step III: Empirical Mode Decomposition (EMD; Huang et al. 1998; Wu and Huang 2004; Wu et al. 2007; Wu and Huang 2009) is then used to break the long record into intrinsic oscillating modes, each with time-dependent amplitude and frequency, and a long-term trend. Even though the original data is at monthly intervals, for the EMD analysis, it appears as if the sampling time interval is $1/M$ month, where M is the number of points along the section. As an example of step I, if $M = 100$, “apparent sampling interval” is increased from monthly data to about 7-h intervals. High-frequency EMD modes with “apparent period” less than 1 month will represent spatial variability within the section, resolving spatial scales between $\sim 5^\circ$ (~ 500 km) and the section’s length (100° or $\sim 10,000$ km in the example above). (Theoretically, the smallest resolved scale according to the Nyquist frequency criteria is 2° , but practically, with this coarse resolution data, smaller scales may be less reliable). The low-frequency modes will represent temporal variability (capturing time scales of a few months to multidecadal), where the EMD is served in effect as a low-pass filter that removes the spatial variability. The approach may be equivalent to an ensemble

of time series at multiple locations, but instead of using standard statistics (e.g., mean and standard deviation over ensemble members), EMD is used as a filter. Therefore, the time series is represented by the EMD as

$$\eta'(t) = \sum_{i=1}^k C_i^S(t) + \sum_{i=k+1}^I C_i^T(t) + r(t) \quad (2)$$

where I is the total number of oscillating modes, C^S and C^T represent spatial and temporal modes, respectively, and r is the long-term trend. The EMD has been used in numerous studies to separate different time scales of sea level variability (Ezer and Corlett 2012; Ezer et al. 2013; Ezer 2015), and EMD was also compared with wavelet analysis (Ezer and Dangendorf 2020), but only temporal modes were considered in those studies. The representation of both spatial and temporal variabilities on the same type of EMD modes allows calculations of relative energy distribution between spatial and temporal variabilities, as demonstrated in the next section. The method developed by Wu and Huang (2004) to calculate energy as a function of frequency and to estimate confidence levels of EMD modes using white noise ensemble calculations was implemented here. The EMD treats spatial and temporal modes the same way and the conversion of units between frequency domain and wavenumber domain is quite simple: for spatial modes, the sampling interval is 1° so the EMD “frequency” output is actually a wavenumber in units of $1/1^\circ$, while for temporal modes, the EMD frequency output divided by N (N = number of points along a section in each month) will be the frequency in $1/\text{month}$ units. The EMD does not distinguish between spatial ($i \leq k$) and temporal ($i > k$) modes, but k is simply chosen by the user such that wavelength for spatial modes is shorter than the section length or that period of oscillations for temporal modes is larger than 2 months. Note that EMD is a nonstationary analysis, so each mode has time-dependent amplitude and frequency, so when showing energy versus frequency, the mean frequency of each mode is often used. However, we found that using median frequency (and thus median period) instead of mean is a more reliable measure, as it eliminates biases due to a few outstanding values.

3 Results

3.1 Spatiotemporal variability of sea level in the Pacific Ocean

The method described above is first tested on two zonal sections across the Pacific Ocean, one at 0.5°N in the equatorial region, and one at 36°N in mid-latitudes (Fig. 1). When

looking at all the points in the two sections (step I of the analysis), they show very different spatial and temporal variations. Kinetic energy and eddy activities are expected to change strongly with latitudes, especially in the Pacific (e.g., Liu et al. 2012), but also in other ocean basins. The equatorial section (Fig. 1a) has persistent east to west sea level slope when warmer waters pile up on the western Pacific side, while the mid-latitude section (Fig. 1b) is dominated by small-scale spatial variations in the western side associated with the Kuroshio Current, but no apparent slope across the rest of the section. The sea level anomaly (step II of the analysis) shows increased spatial variability in eastern equatorial regions (Fig. 1c), compared with more variability in the western mid-latitudes (Fig. 1d). The time series that include all the spatial and temporal data of Fig. 1c and Fig. 1d are shown in Fig. 1e and Fig. 1f, respectively; both show increased variability with time, a result that is consistent with the increased kinetic energy discussed in Ezer and Dangendorf (2021) and other recent studies. The El Niño events are seen (red start in Fig. 1e) as peaks when spatial sea level differences across the equatorial Pacific are unusually large and increased since the 1980s. The largest 2 signals seen in Fig. 1e coincide with the 2 strongest El Niño events in 1983 and 1998 (<https://psl.noaa.gov/enso/>); the strong La Niña at the end of 1998 may also contribute to this large signal. The nonlinear sea level rise is also apparent in both locations (black lines in Fig. 1e and Fig. 1f).

In the last part of the analysis (step III above), the combined energy of spatial and temporal variabilities was calculated, showing remarkable differences between the two locations. In the equatorial section (Fig. 1g), there is almost no energy in spatial variability, but large and statistically significant energy (above 99%) at temporal variability in time scales between 3 months and 60 years. Energy in the mid-latitude section (Fig. 1h) is exactly the opposite, with maximum relative energy at spatial variability at scales of ~ 500 – $10,000$ km but diminished temporal variability except for time scales over 20 years. Note that the EMD can detect statistically significant long-term oscillations of only a few cycles because they are based not on a single point or mean sea level, but on 100 s of points along a single section where all points contribute to the statistics. In some sense, our method is equivalent to an ensemble of simulations with many sampling data points, using the EMD to filter out spatial variations when detecting long-term temporal variability.

3.2 Spatiotemporal variability of sea level in the Atlantic Ocean

The information provided by the new analysis was demonstrated above for two sections across the Pacific Ocean, showing very significant differences in spatiotemporal characteristics between the sections. Therefore, nine sections

Sea level variability across the Pacific Ocean 1900-1915

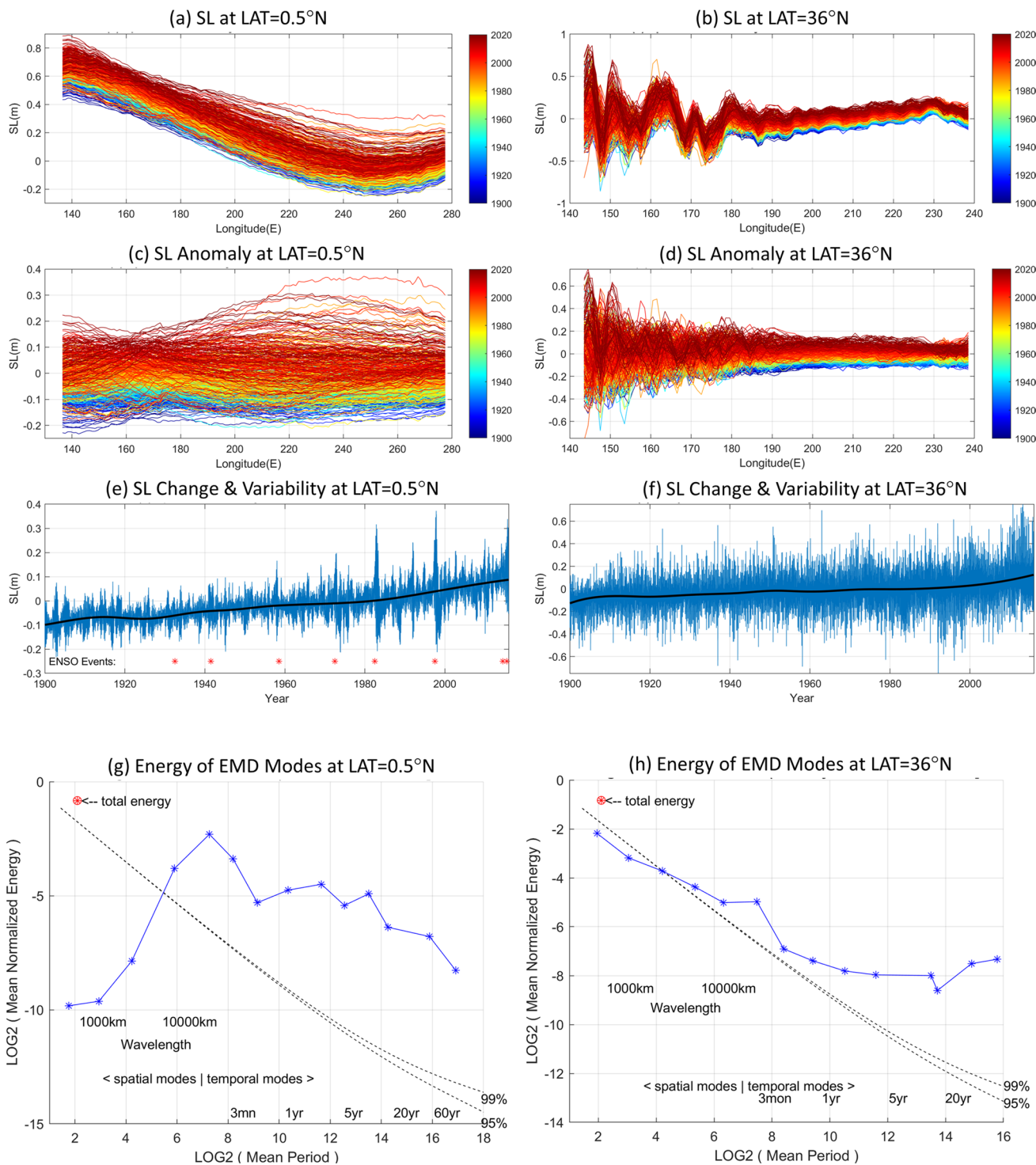
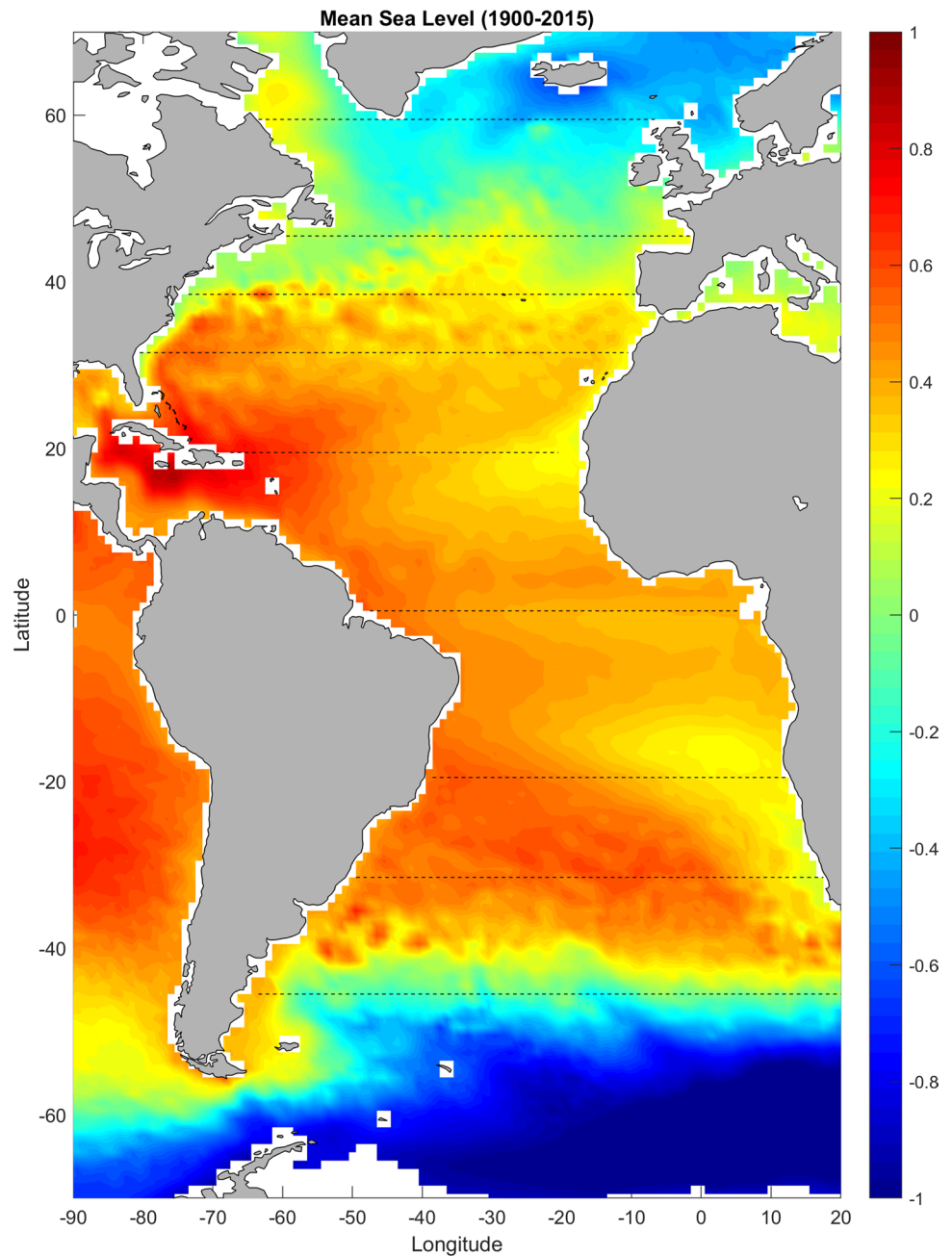


Fig. 1 Demonstration of the spatiotemporal analysis of variability along zonal cross sections: Pacific Ocean at 0.5°N (left panels) and 36°N (right panels). Top panels: monthly sea level versus longitude and time (color); second panels: sea level anomaly (local time-mean was removed); third panels: sea level change (spatial and temporal,

including all points are in blue, and trends in black); bottom panels: relative energy of EMD modes and their mean period (the highest frequency modes represent spatial variations, as indicated). Figure 1e shows El Niño events (red stars) which coincide with peaks in sea level variability

Fig. 2 Mean sea level (in m) in the Atlantic Ocean (RecSL 1900–2015) and zonal cross sections used in this study



across the Atlantic Ocean (Fig. 2) are investigated to further understand the latitudinal distribution of variability; these sections were selected to represent different major ocean currents, to demonstrate the different variability in each section. The analysis will also be used to compare the RecSL with gridded altimeter data which were interpolated to the same grid as the RecSL data. The altimeter record is only 23-year long compared with the 116-year long RecSL record, so most of the early years of the reconstruction rely mostly on tide gauge data. Because of the significant difference in record length between the two data sets (one is 5 times longer than the other one), comparison of variability

in the two records using standard spectral analysis methods would be possible only for the overlapping 23-year period and would result in limited information regarding the lower frequencies. On the other hand, it will be shown below that the new analysis method can overcome this problem, using the full length of the two records.

3.2.1 Comparison between altimeter data and sea level reconstruction

Figure 3 compares 5 sections of RecSL and altimeter data across the North Atlantic Ocean. First, it is interesting to note

the similarity between the Pacific and Atlantic Oceans' sections when comparing similar latitudes (Fig. 1a and b versus Fig. 3e and i). Second, the difference in spatial sea level variations at different latitudes is quite astounding, from smooth equatorial slope across the whole basin (Fig. 3i), to wave-like sea level (wavelength of ~6 degrees) at 32°N (Fig. 3g), to sharp fronts and recirculation cells near the Gulf Stream at 39°N and 46°N (Fig. 3e and c) and the slope across the Labrador Current at 60°N (Fig. 3a). A third qualitative result is the similar variability seen in the RecSL and altimeter data. Apparently, ocean currents and thermal features that affect spatial sea level variations are seen at similar locations across each section, though variations are somewhat larger in the altimeter data than the RecSL data—for example, sea level change across the Gulf Stream between 60°W and 65°W is ~1.7 m in the altimeter data and ~1.2 m in the RecSL data (Fig. 3e and f). An interesting result is that despite sea level rise and the potential of changes in variability over time, spatial variations in each section remain locked to the same locations throughout the century of RecSL data, pointing to semi-permanent circulation patterns that may be locked with topographical and thermal features. Since the altimeter data shows a very similar pattern of wave-like spatial features as seen in the RecSL record, this pattern does not seem an artifact of the spatial EOF modes used in the RecSL reconstruction.

To further compare the RecSL and altimeter data, the relative energy distribution between spatial and temporal variabilities is shown in Fig. 4. Despite the huge difference in the length of the two records (the RecSL record is 5 times longer than the altimeter record), the latitudinal changes in spatiotemporal variability are surprisingly very similar. Except oscillations with periods longer than ~20 years that are unresolved in the shorter altimeter record, at all other spatial and temporal scales, the same pattern appears in both, the RecSL and the altimeter data, with increased spatial variability (high-frequency) in mid-latitudes (Fig. 4c–h) and relatively more energy at temporal variability at high latitudes (Fig. 4a–b) and equatorial regions (Fig. 4i–j). The fact that even the relatively short record of the altimeter data was able to represent most of the spatiotemporal variability seen in the century-long RecSL record is attributed to the nature of the analysis, which used many points along each section to increase the number of degrees of freedom. If instead, a standard spectral analysis of section-mean sea level was done, the spectrum of 23 years of altimeter data could not be compared with the spectrum of 116 years of RecSL data, since they resolve completely different windows of frequencies. While it should be acknowledged that the altimeter and RecSL data are not completely independent of each other (spatial patterns in the altimeter data were used in the construction of the RecSL data), the comparison using the new analysis method demonstrated that the analysis method is quite robust.

3.2.2 Latitudinal variations in spatial and temporal variability

Examples of the spatial variability of the smallest resolved scales were obtained from the first EMD mode ($i=1$ in Eq. 2) and are shown in Fig. 5. The typical wavelength of this mode is ~6–7 degrees (~400, 500, 550, and 600 km for latitudes 60°N, 46°N, 39°N, and 32°N, respectively). The maximum spatial variability is seen near the Gulf Stream at 39°N (Fig. 5c) while smaller variability is seen at 32°N (Fig. 5d; subtropical gyre) and 60°N (Fig. 5a; subpolar gyre). (The equatorial section, not shown, also has minimal spatial variability as shown in Fig. 4.) An interesting result is a general increase in variability over time, especially in low to middle latitudes (Fig. 5b–d) and less so at 60°N (Fig. 5a). Since this increase started many years before altimeter data were used, this trend cannot be attributed solely to the recent inclusion of satellite data in the reconstruction. In fact, several studies indicate an intensification of surface currents over time in the global ocean with changes especially visible near western boundary currents (Deser et al. 1999; Cai 2006; Yang et al. 2016; Chen et al. 2019; Hu et al. 2020; Sen Gupta et al. 2021). Recent studies showed, for example, that climatic changes may affect local wind stress curl, and can also induce uneven warming of ocean temperatures, increase spatial gradients, and increase kinetic energy over time (Ezer and Dangendorf 2021). Some observations of surface temperatures and altimeters confirm that eddy activities are increasing near WBCs (Martínez-Moreno et al. 2021); the results here of increased spatial variability are consistent with these findings.

Examples of the low-frequency temporal variability are shown in Fig. 6 for the same four sections of Fig. 5; these are the 3 EMD oscillating modes with the lowest frequency ($i=I-2, I-1, I$, in Eq. 2; modes 11–13 in Fig. 6) and the trend r . The mean periods of these modes range between 6 and 60 years, but it is clear that these are nonlinear nonstationary variations where the amplitude and frequency vary with time. The nonlinear trend is also different at each latitude, showing recent sea level acceleration at 32°N and 46°N (Fig. 6b and Fig. 6d), but deceleration at 39°N and 60°N (Fig. 6a and Fig. 6c). No coherent oscillations between latitudes are seen; in fact, mode 13, for example, shows that after 2000, sea level changed in opposite direction at 32°N versus 39°N and in opposite direction at 46°N versus 60°N, which could happen when the subtropical gyre or the subpolar gyre intensifies or weakens.

Figure 7 summarizes the spatiotemporal variability at the 9 Atlantic cross sections shown in Fig. 2, comparing the relative energy at different modes (relative to total energy on a log₂ scale; see Fig. 4). Energy at temporal scales of few months to few years (Fig. 7b) shows relative insensitivity to latitude, except for some increased energy at high latitudes

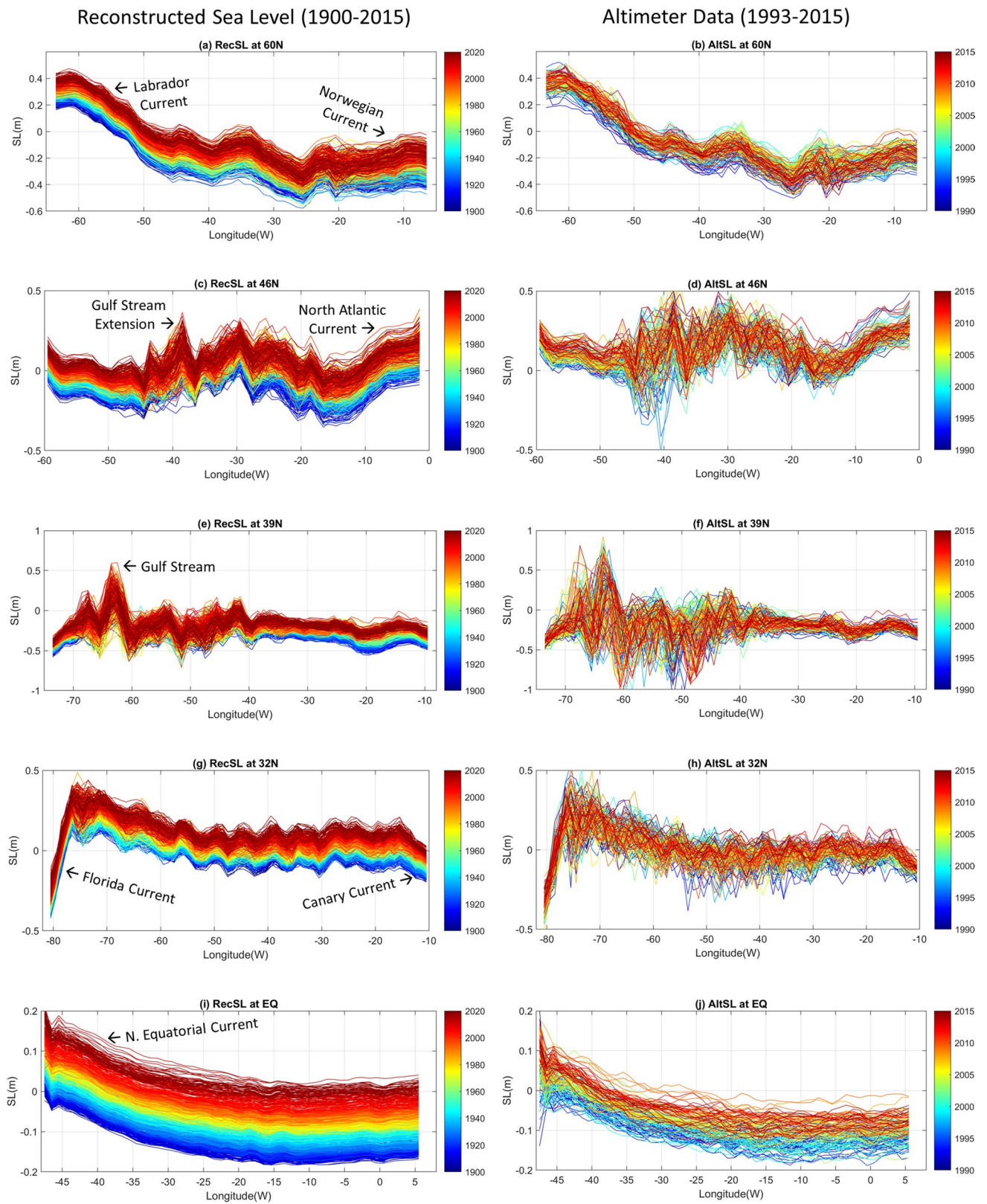


Fig. 3 Comparison of sea level at different North Atlantic zonal cross sections between RecSL (left panels; 1900–2015) and altimeter data (right panels; 1993–2015), as in the top panels of Fig. 1. Some ocean

currents associated with spatial slopes are indicated in the left panels. Note the different color scales of the two data sources

Fig. 4 Comparison of energy in EMD modes (as in bottom panels of Fig. 1) in the North Atlantic (same cross sections as Fig. 3) for RecSL (left panels) versus altimeter data (right panels)

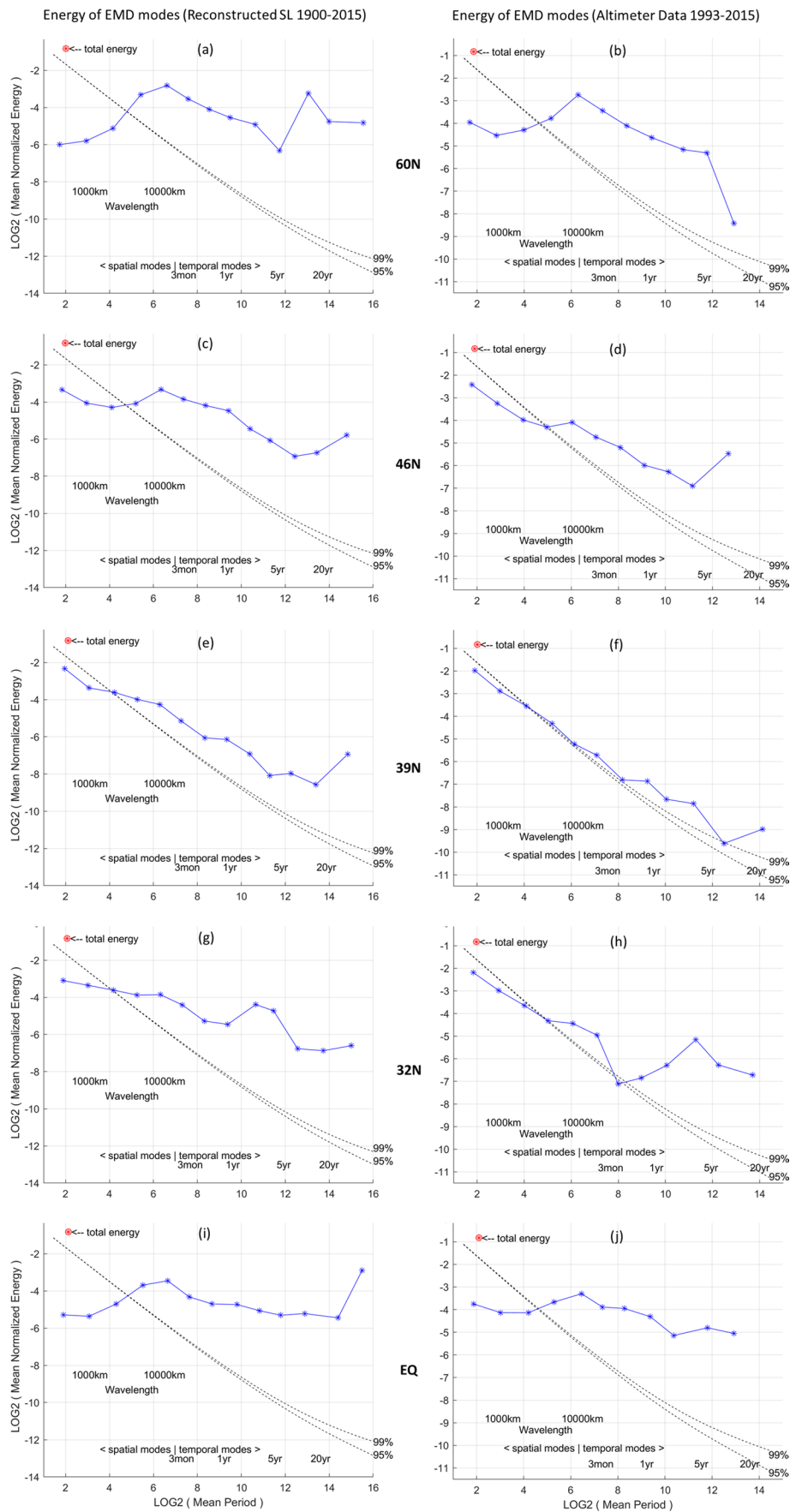
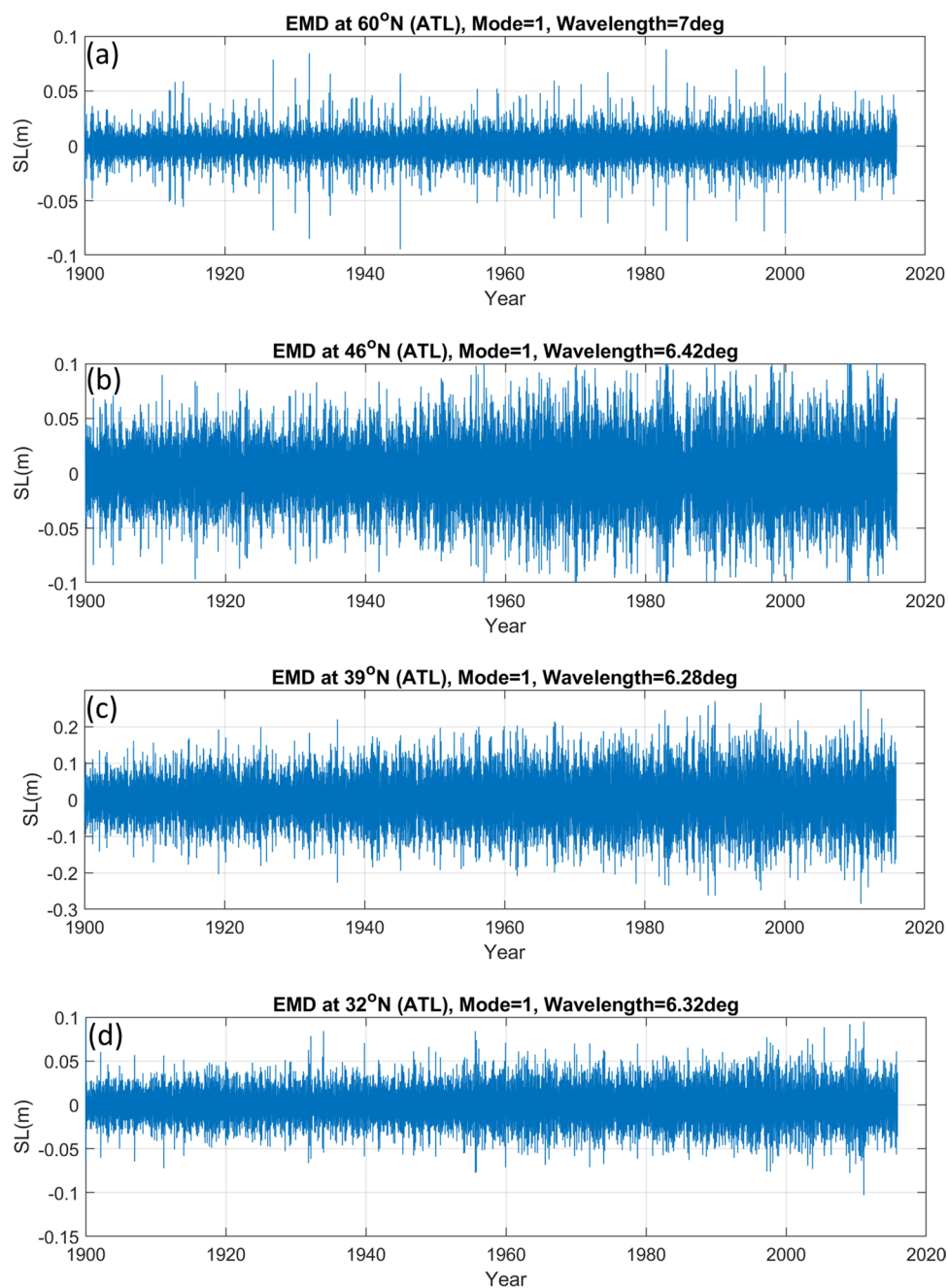


Fig. 5 Examples of the highest frequency EMD modes in North Atlantic sections, representing spatial variability (mean length scale in degree longitude is indicated)



(46°N and 60°N). However, large latitudinal differences are evident for energy distribution between the smallest spatial scales (Fig. 7a) and the longest temporal scales (Fig. 7c). Two regions stand out in particular—near the Gulf Stream and the Antarctic Circumpolar Current long-term temporal variability is especially low, while most of the energy is in mesoscale spatial variability. On the other hand, diminished spatial variability and increased long-term temporal variability are seen in equatorial and the subpolar North Atlantic regions. The latitudinal changes in variability found here are generally in agreement with other studies. Serazin et al. (2015),

for example, found increased variability in mid-latitudes and minimal small-scale variability in tropical regions, pointing to the fact that mesoscale variability in mid-latitudes is intrinsic oceanic instability and less influenced by atmospheric variability which impact mostly long-term variability.

3.2.3 North Atlantic Oscillation (NAO) and its relation to spatiotemporal sea level variability

As seen in Fig. 6, long-term sea level variability and sea level rise are uneven over the Atlantic and the variability

Fig. 6 Examples of low-frequency EMD modes for the four sections of Fig. 5. Modes 11–13 are oscillation modes (median period is indicated) and mode 14 is the trend

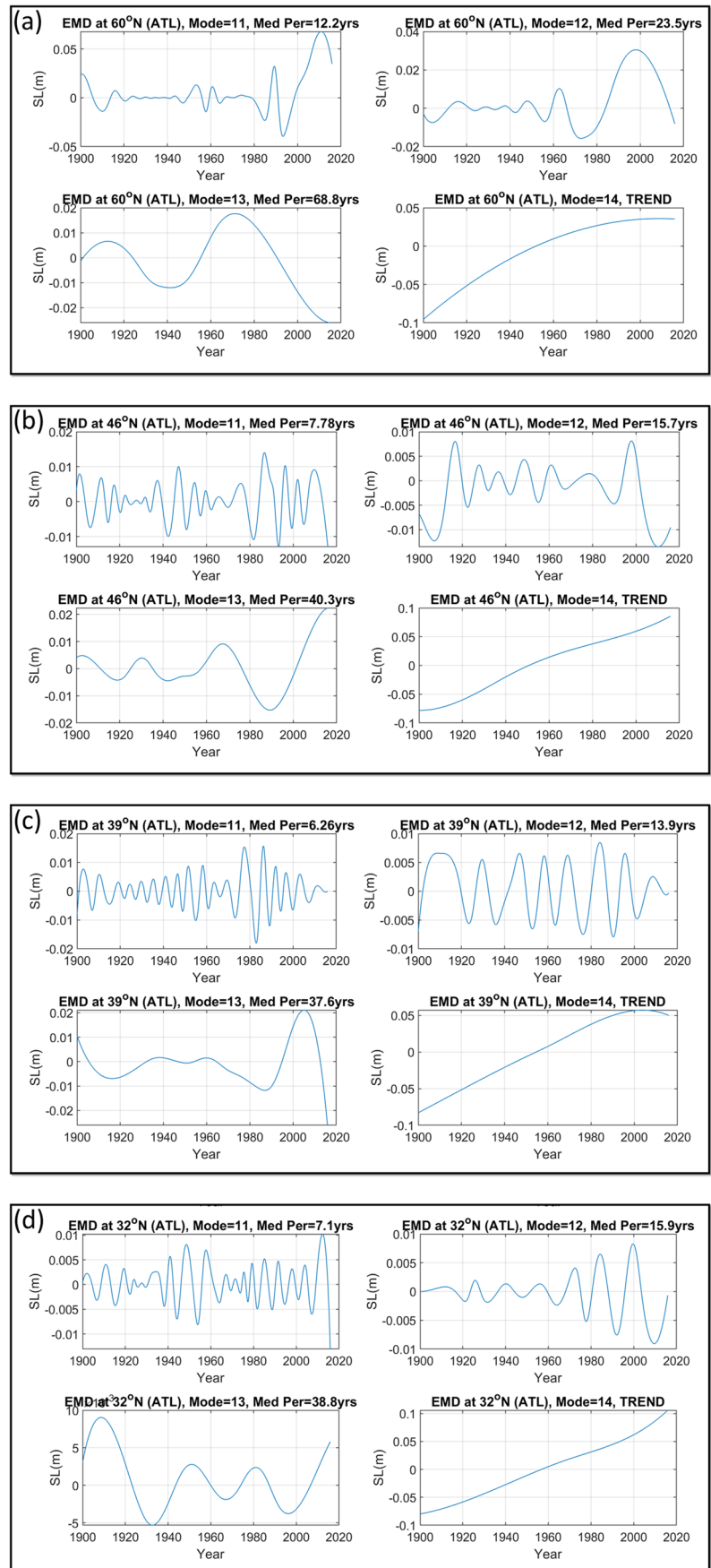
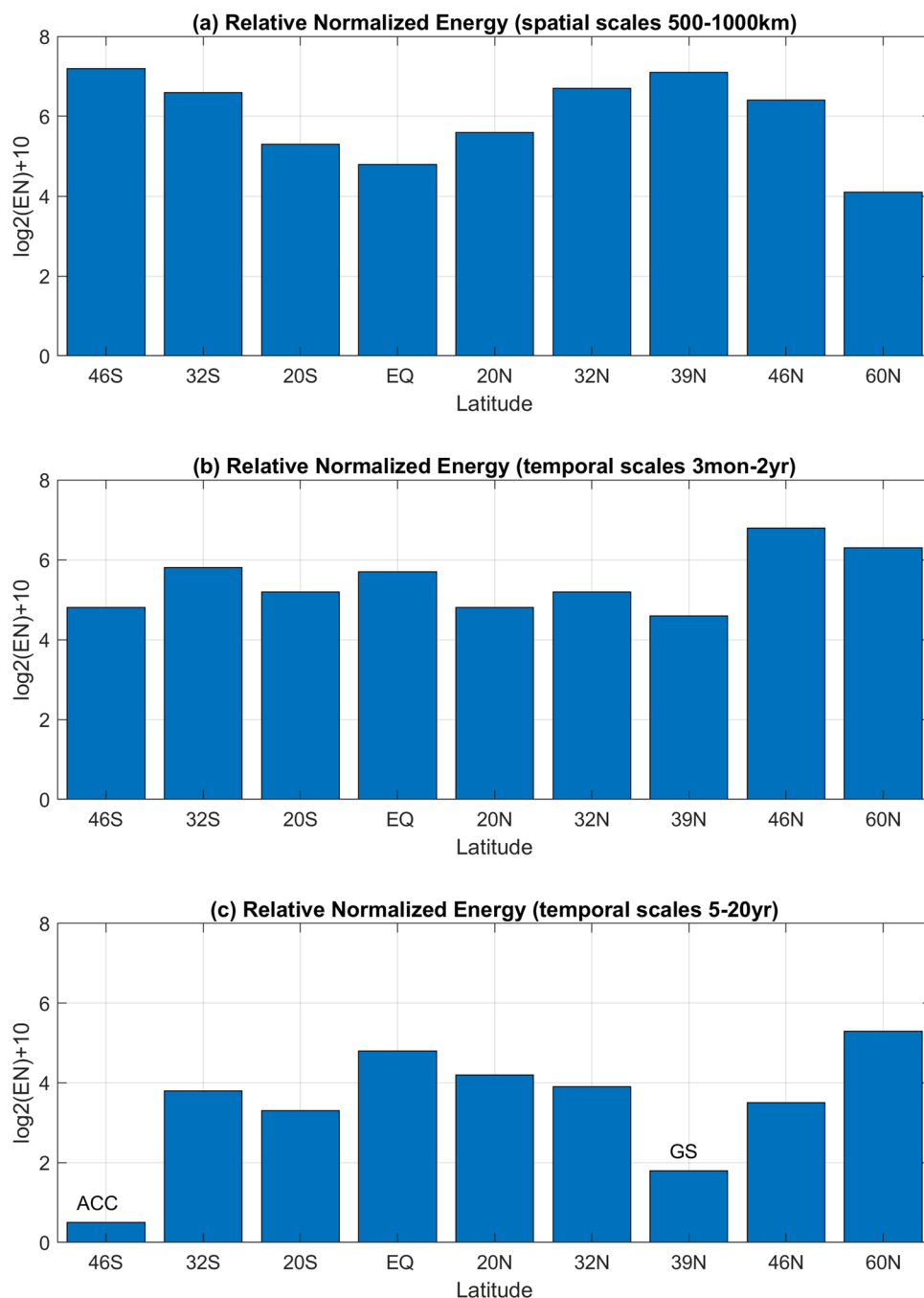


Fig. 7 Relative normalized energy (as in left panels of Fig. 4) at the different sections of Fig. 2 and for different scales: **a** smallest resolved spatial scales (the highest frequency EMD modes 1–2), **b** middle frequencies temporal scales (EMD modes 5–8), and **c** low-frequency temporal modes (EMD modes 10–12). The sections near the Gulf Stream (GS) and near the Antarctic Circumpolar Current (ACC) are distinct in their high energy at small spatial variability and low energy at long temporal time scales



seemed to change for different latitudes and different time scales. While there are many different drivers for regional variations in sea level, one of the main features that links these drivers is the North Atlantic Oscillations (NAO) which is linked with changes in wind patterns, the Gulf Stream, sea level rise, and AMOC (Taylor and Stephens 1998; Joyce et al. 2000; Baringer and Larsen 2001; Meinen et al. 2010; McCarthy et al. 2012; Ezer 2015; Ezer et al. 2016; Ezer and Dangendorf 2020, 2021). Figure 8 shows the mean sea level rise and sea level variability over the Atlantic Ocean and the annual NAO index (Hurrell 1995; Hurrell et al. 2003;

data obtained from the UCAR web site <https://climatedataguide.ucar.edu/climate-data>). The uneven sea level rise, with deceleration between the 1940s and 1960s and increase acceleration after the 1960s (Fig. 8b) and its relation to ice melt, water storage, and wind shifts, has been discussed recently in several studies (Dangendorf et al. 2014, 2017, 2019; Frederikse et al. 2020; Ezer and Dangendorf 2020, 2021). Qualitatively, low-frequency variations in NAO tend to be anticorrelated with low-frequency variations of mean sea level over the entire Atlantic (Fig. 8c), with higher sea level during periods of lower (or negative) NAO and vice

versa, but for decadal and longer time scales, these correlations are not so accurate. This relation is likely to be associated with different mechanisms at different time and length scales, as regional studies show for example for the subtropical region (Joyce et al. 2000) or the Gulf Stream (Ezer 2015). Therefore, analysis of the spatiotemporal impact of NAO on sea level was conducted next.

The annual NAO index for 1900–2015 was first decomposed into EMD modes (Fig. 9) showing median periods of oscillated modes ranging from ~6 to ~50 years and a non-linear trend indicating acceleration. Some modes are very nonstationary, such as mode 4 with increased oscillations since the 1990s, while other modes show a steady oscillation, such as mode 5 with a 48-year cycle. At this point, the EMD modes do not necessarily indicate specific processes, so the EMD modes are divided into 4 groups: interannual time scales of about 5–10 years (modes 1 + 2), decadal time scales of about 15–25 years (modes 3 + 4), multidecadal time scales of about 50 years (mode 5), and the long-term trend. After the linear sea level rise trend was removed from each point, correlations between the annual sea level anomaly and the annual NAO index at all points were calculated for the 4 groups of modes (Fig. 10). Since, unlike sea level rise, there is no persistent long-term trend in NAO, a comparison must be made with linearly detrended sea level. Note, however, that long-term nonlinear variations in sea level that contribute to the trend remain (Fig. 10d). For the original record of 116 years, a significance level of 95% is achieved for correlation $|R| > 0.18$, but since low-frequency modes have smaller degrees of freedom, a higher correlation is needed for the same significance (Ezer 2015; Ezer et al. 2016; Ezer and Dangendorf 2020), so for example, correlations of ~0.3–0.4 would be needed for 95% confidence when correlating two time series that include only decadal modes. Note, however, that except the removal of trend, the sea level data was not filtered or decomposed into modes, because the main goal is to qualitatively assess the spatiotemporal link between NAO and sea level, i.e., to see what part of the full spectrum of annual sea level variability is linked with what NAO time scales and at what geographical locations. The results indicate that variations in NAO at each of the four time scales are linked with sea level variability at different locations. Interannual variations in NAO (Fig. 10a) are highly positively correlated with sea level at the subpolar gyre, the Nordic Seas and the North Sea, but negatively correlated with sea level along the US East Coast north of Cape Hatteras. In fact, at all scales, the US coastal sea level is negatively correlated with NAO, which agrees with numerous studies that showed higher coastal sea level when the NAO is low, which can result in increased coastal flooding, as was the case during 2009–2010 (Ezer 2015; Goddard et al. 2015). For decadal variability, the highest negative correlation was found in equatorial and tropical regions (Fig. 10b); for multidecadal

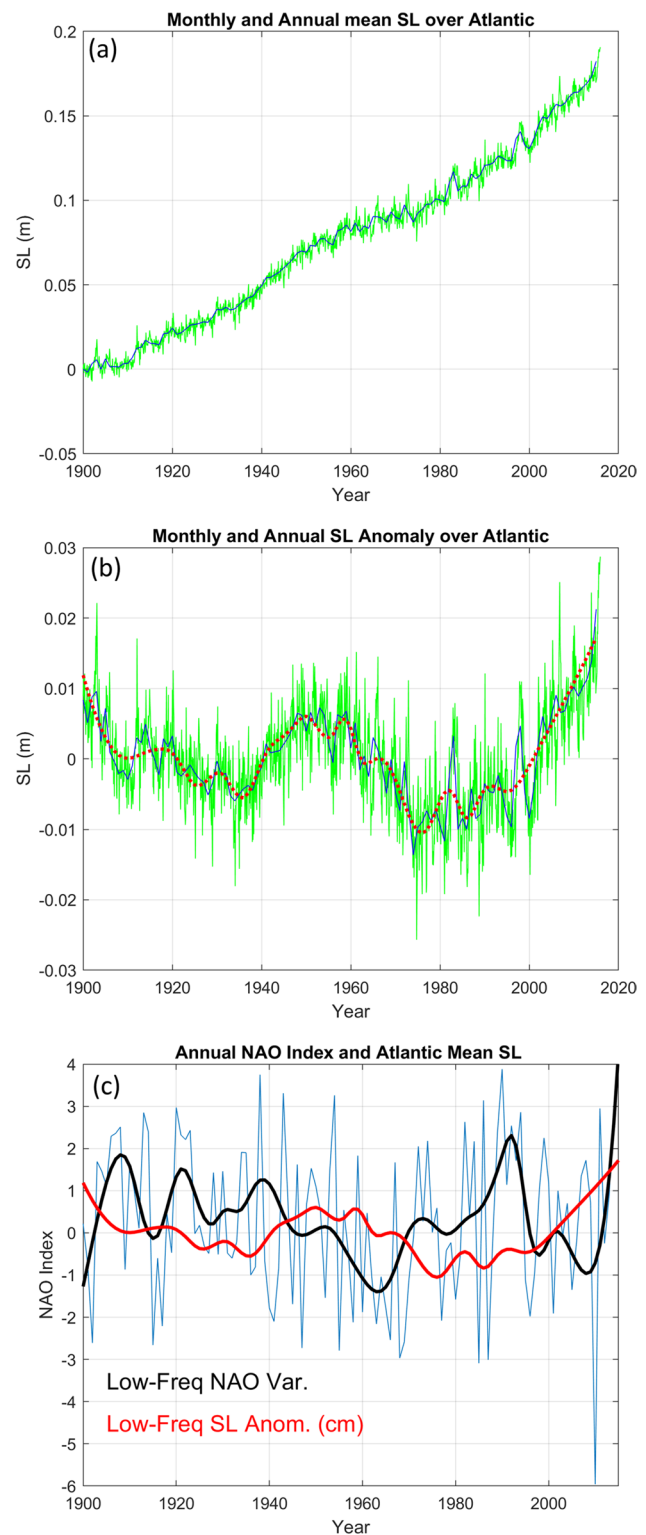
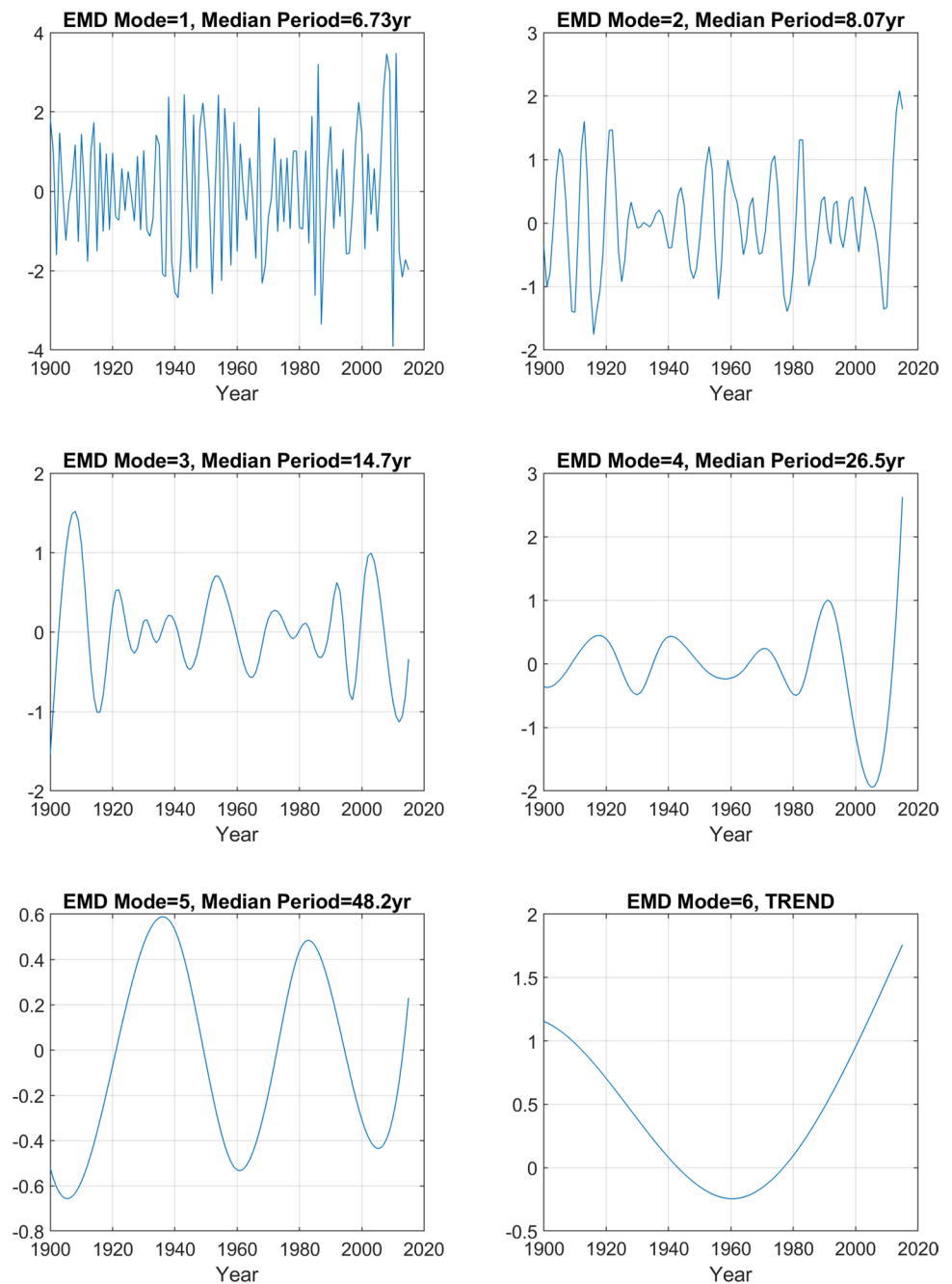


Fig. 8 Mean sea level over the area shown in Fig. 2 (mostly the Atlantic Ocean): **a** Monthly (green) and annual (blue) sea level change since 1900 and **b** monthly and annual sea level anomaly (linear trend and area mean were removed); low-passed filtered line (red dotted) is the sum of low-frequency EMD modes. **c** Annual NAO index (blue) and its low-frequency EMD modes (black) are compared with the low-frequency EMD modes of sea level (red)

Fig. 9 EMD modes of the annual NAO index of Fig. 8c. The median period of each oscillating mode (EMD 1–5) is indicated



variability (Fig. 10c), a significant negative correlation was extended to the southern equatorial region and the Southern Ocean off Antarctic. Only the correlation of multidecadal modes (Fig. 10c) shows quite homogeneous negative correlation over most of the Atlantic Ocean, suggesting that the 48-year cycle (Fig. 9) is likely a basin-wide oscillating mode. Correlation of sea level with the NAO trend indicates a positive correlation near Iceland and near Antarctica, which may suggest some barostatic-dynamic response to ice melt at high latitudes or response to climatic wind shift in the Southern Ocean (Cai 2006; Dangendorf et al. 2019; Ezer

and Dangendorf 2021). Since linear trend was removed from sea level and the NAO showed an acceleration in its long-term trend (Fig. 9), a positive correlation in Fig. 10d indicates regions with local acceleration in sea level (however, statistical significance between smooth trend lines is low, so one should only consider the results qualitatively in this context). Finding the exact mechanisms of the basin-wide link between NAO and sea level is beyond the scope of this study, which aimed to demonstrate the complex spatiotemporal nature of the variability. However, there are clearly several mechanisms involved, including the path of weather

systems, SST and wind shifts, and global barostatic impacts, and it is possible that the correlation does not indicate a simple cause and effect, but rather a basin-wide air-sea-ice coupled modes that impact both NAO and sea level variability. Further analysis and sensitivity studies with climate models would help to understand the different mechanisms.

4 Summary and conclusions

The study introduced and tested a new analysis method to study spatiotemporal sea level variability. The method can be useful for any model or observed data that involve space and time such as along-track satellite data or repeated model or observations along sections. A proof-of-concept demonstration was conducted here with examples of sea level variability in the Pacific and the Atlantic Oceans, but this analysis can be used for other oceans and other data such as sea surface temperature or various climate data. More traditional spatiotemporal approaches that have been used for a long time such as SVD (Mann and Park 1996) or EOF (Oey et al. 2004) separate data into spatial patterns and their time-dependent time evolution, or extract variability in a frequency-time domain such as wavelet analysis (Grinsted et al. 2004). In other methods, spatiotemporal variability at windows of interest is extracted by applying space and time filters (Serazin et al. 2015). None of those methods treat the spatial and temporal variabilities the same way as done here, so the idea behind our approach was to find a way to directly compare energy embedded in spatial variability with energy embedded in temporal variability. Another advantage of the new method is that combining space and time measurements into one long time series provides significantly more data points than analyzing for example just means values. For example, if one is interested in temporal variability, our analysis of a cross section of 100 spatial points is like an ensemble of 100 time series, which provides a more accurate result than analyzing a single point. Note, however, that because the points along a section are not independent estimates, the increase in the number of degrees of freedom compared with a single time series would be somewhat less than 100 times. Similarly, if one is interested in the spatial variability, our analysis of an ensemble of 1392 monthly Sects. (116 years times 12) would provide much greater accuracy than analysis of a single section. The analysis is thus a type of ensemble statistics using the EMD to filter out (low frequency) temporal modes when extracting spatial variability and to filter out (high frequency) spatial modes when extracting energy of temporal modes. While the EMD does not distinguish between spatial and temporal modes, conversion from frequency (and period) to wavenumber (and wavelength) is straightforward given the interval in time (monthly data) and space (1 degree longitude). Practically,

high-frequency EMD modes with “apparent period” less than 1 month will represent spatial modes. The long-term trend includes contributions from all points along the section, whereas the EMD filters out all the oscillating modes. Because of the exceptionally long record of the combined spatial and temporal data, oscillation modes with periods up to ~40 years are statistically significant in the 116-year long RecSL when using white noise ensemble tests developed by Wu et al. (2004, 2009). A test of the robustness of the methods compared 23 years of altimeter data with 116 years RecSL data and showed that (1) the analysis detected almost identical spatial and temporal modes in both data except time scales longer than ~20 years in the altimeter data and 2. The latitudinal change in the relative energy of spatial versus temporal modes in the two data sets was very similar. Both data sets showed relatively higher energy in spatial modes in mid-latitudes and in regions with strong currents such as the Kuroshio, the Gulf Stream, and the ACC, but less spatial variability and relatively higher energy in low-frequency temporal modes in tropical and in subpolar regions. The similarity between the analysis of the two records with so different lengths shows the advantage of the method over other analyses such as spectral approaches or wavelets which will result in energy at very different frequencies if one tries to compare two time series, when one of them is 5 times longer than the other.

The latitudinal and geographical distribution of variability in the Atlantic Ocean and their connection to NAO modes were investigated with the help of the spatiotemporal analysis. Some interesting results include the increased spatial variability over time, which is consistent with some studies that show increased kinetic energy near western boundary currents (Deser et al. 1999; Chen et al. 2019; Yang et al. 2016; Martínez-Moreno et al. 2021) under warmer climate conditions. Another finding is the large difference in spatial variability between tropical regions that almost lack any mesoscale variability and subtropical and mid-latitudes that show semi-permanent spatial wave-like pattern (wavelength of ~6–7°; see Fig. 3g) that remains throughout the last century; thus, these patterns may not be due to propagating eddies or Rossby waves, but rather small-scale flow patterns locked to topography. Long-term variability (time scales ~8–40 years) was also found to be very different at different latitudes in the Atlantic Ocean. Sea level rise trend is also strongly latitudinal-dependent, showing for example recent acceleration at 32°N but deceleration at 39°N, suggesting a possible shift in subtropical ocean currents (Ezer and Dangendorf 2020, 2021). The link between NAO and spatiotemporal sea level variability has been demonstrated. It is noted that links between NAO and sea level have been shown before, for example, for European coasts (Chen et al. 2014; Dangendorf et al. 2014; Tsimplis et al. 2013; Ezer et al. 2016) and North American coasts (Ezer 2015; Ezer

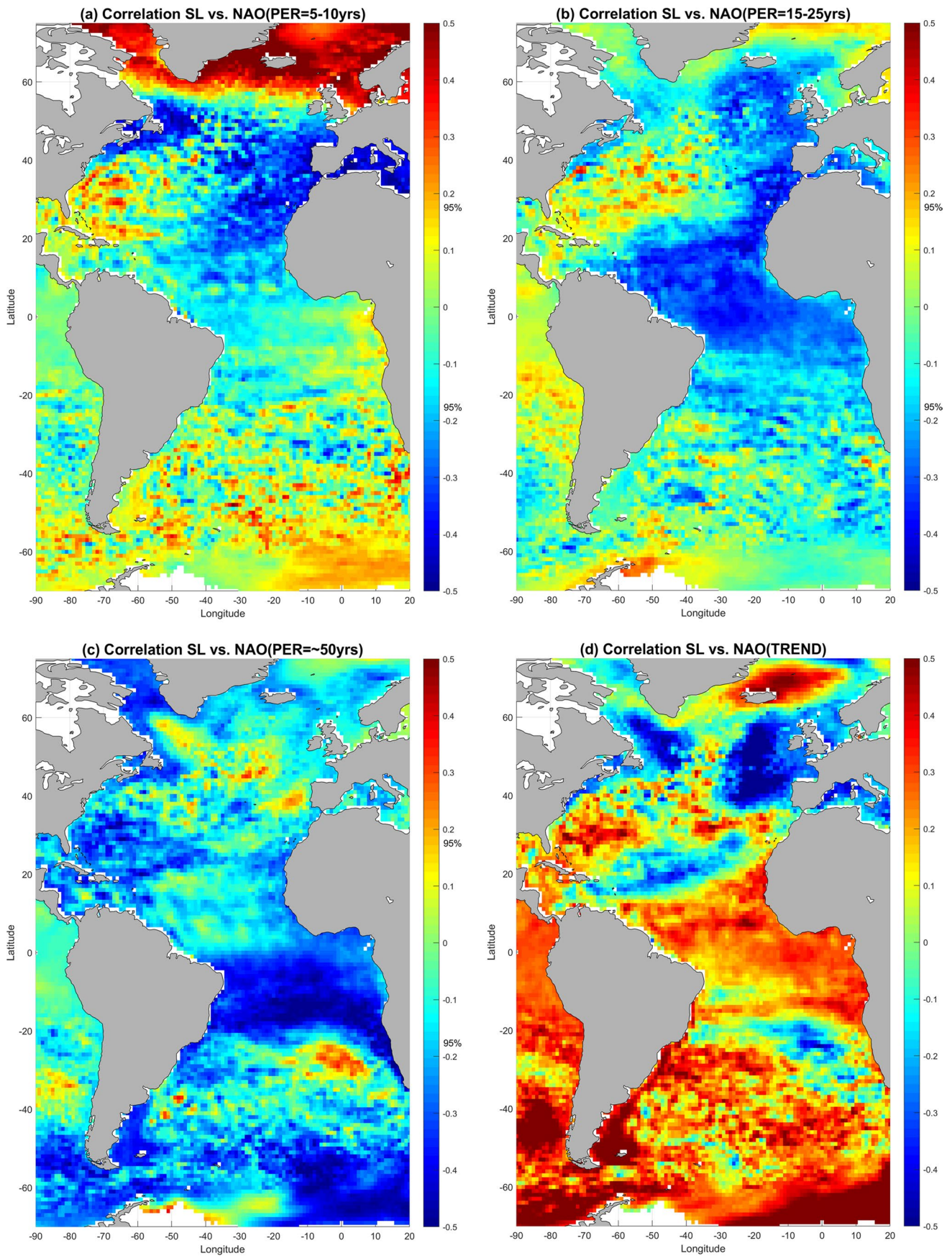


Fig. 10 Correlation between detrended sea level anomaly (1900–2015) and EMD modes of NAO (Fig. 9): **a** modes 1+2 (time scales ~5–10 years), **b** modes 3+4 (time scales ~15–25 years), **c** mode 5 (time scales ~50 years), and **d** mode 6 (NAO trend). Correlations over 95% confidence level are the darkest red (positive correlation) and blue (negative correlation). Statistical significance of the trend in **d** is unclear

et al. 2013, 2016; Kenigson et al. 2018). While most of the previous studies focused on interannual variations in the North Atlantic, we expand the scope to longer time scales in our century-long record; links with the South Atlantic were also found. The results show that on interannual time scales, low NAO index is linked with low sea level in the subpolar region, but increased sea level along the western North Atlantic coasts (a result consistent with Ezer 2015; Goddard et al. 2015, and others); however, on decadal and multidecadal time scales, low NAO is most closely linked with increased sea level in tropical and Antarctic regions. The 116-year long-term trend of NAO indicates a general decline for 1900–1960 and an upward trend for 1960–2015 (Fig. 9). While the statistical significance of this trend is not clear given the record length, it appears that this trend is positively correlated with sea level anomaly near Iceland and along the Antarctic coast, suggesting a possible link to high latitude ice melt.

This study was aimed to demonstrate the potential of this new analysis and to provide tools that can be used to investigate spatiotemporal variability in different observations and model results. The approach is somewhat different than traditional spatiotemporal approaches such as SVD, EOF, or wavelet since energy in spatial and temporal variabilities is simultaneously analyzed and directly compared instead of separated. Further evaluation with other data is clearly needed. The method is especially useful for repeat section data, such as along-track satellite data.

The study is part of Old Dominion University's Climate Change and Sea Level Rise Initiative at the Institute for Coastal Adaptation and Resilience (ICAR).

Acknowledgements The Center for Coastal Physical Oceanography (CCPO) provided facility and computational resources. Two anonymous reviewers are thanked for useful suggestions that helped improve the manuscript.

Data availability The NAO index is available from UCAR (<https://climatedataguide.ucar.edu/climate-data/hurrell-north-atlantic-oscillation-nao-index-pc-based>), the altimeter data is available from the Copernicus Marine service (<https://marine.copernicus.eu/>) and the RecSL data is available by request from the authors. The data used are publicly available from the links provided and the reconstruction is available by request from the authors.

Declarations

Conflict of interest The authors declare no competing interests.

References

- Andres M, Donohue KA, Toole JM (2020) The Gulf Stream's path and time-averaged velocity structure and transport at 68.5°W and 70.3°W. *Deep-Sea Res Part I* 156. doi:<https://doi.org/10.1016/j.dsr.2019.103179>
- Baringer MO, Larsen JC (2001) Sixteen years of Florida current transport at 27°N. *Geophys Res Lett* 28(16):3179–3182. <https://doi.org/10.1029/2001GL013246>
- Beal LM, Elipot S (2016) Broadening not strengthening of the Agulhas current since the early 1990s. *Nature*. <https://doi.org/10.1038/nature19853>
- Blaker ET, Hirschi JM, McCarthy G, Sinha B, Taws S, Marsh R, Coward A, de Cuevas B (2014) Historical analogues of the recent extreme minima observed in the Atlantic meridional overturning circulation at 26°N. *Clim Dyn* 44(1–2):457–473. <https://doi.org/10.1007/s00382-014-2274-6>
- Bryden HL, Longworth HR, Cunningham SA (2005) Slowing of the Atlantic meridional overturning circulation at 25°N. *Nature* 438:655–657. <https://doi.org/10.1038/nature04385>
- Caesar L, Rahmstorf S, Robinson A, Feulner G, Saba V (2018) Observed fingerprint of a weakening Atlantic Ocean overturning circulation. *Nature* 556:191–196. <https://doi.org/10.1038/s41586-018-0006-5>
- Cai W (2006) Antarctic ozone depletion causes an intensification of the Southern Ocean super-gyre circulation. *Geophys Res Lett* 33:L03712. <https://doi.org/10.1029/2005GL024911>
- Calafat FM, Chambers DP, Tsimplis MN (2014) On the ability of global sea level reconstructions to determine trends and variability. *J Geophys Res* 119:1572–1592. <https://doi.org/10.1002/2013JC009298>
- Chelton DB, DeSzoeke RA, Schlax MG, Naggar KE, Siwertz N (1998) Geographical variability of the first baroclinic Rossby radius of deformation. *J Phys Oceanogr* 28:433–460
- Chen X, Dangendorf S, Narayan N, O'Driscoll K, Tsimplis MN, Su J, Mayer B, Pohlmann T (2014) On sea-level change in the North Sea influenced by the North Atlantic Oscillation: local and remote steric effects. *Estuar Coast and Shelf Sci* 151:186–195. <https://doi.org/10.1016/j.ecss.2014.10.009>
- Chen C, Wang G, Xie S, Liu W (2019) Why does global warming weaken the Gulf Stream but intensify the Kuroshio? *J Clim* 32:7437–7451. <https://doi.org/10.1175/JCLI-D-18-0895.1>
- Church JA, White NJ (2006) A 20th century acceleration in global sea-level rise. *Geophys Res Lett* 33(1). doi:<https://doi.org/10.1029/2005GL024826>
- Church JA, White NJ (2011) Sea-level rise from the late 19th to the early 21st century. *Surv Geophys* 32:585–602. <https://doi.org/10.1007/s10712-011-9119-1>
- Dangendorf S, Rybski D, Mudersbach C, Müller A, Kaufmann E, Zorita E (2014) Jensen J (2014) Evidence for long-term memory in sea level. *Geophys Res Lett* 41:5564–5571. <https://doi.org/10.1002/2014GL060538>
- Dangendorf S, Marcos M, Wöppelmann G, Conrad CP, Frederikse T, Riva R (2017) Reassessment of 20th century global mean sea level rise. *Proc Nat Acad Sci* 114(23):5946–5951. <https://doi.org/10.1073/pnas.1616007114>
- Dangendorf S, Hay C, Calafat FM, Marcos M, Piecuch CG, Berk K, Jensen J (2019) Persistent acceleration in global sea-level rise since the 1960s. *Nat Clim Change* 9:705–710. <https://doi.org/10.1038/s41558-019-0531-8>
- Dangendorf S, Frederikse T, Chafik L, Klinck J, Ezer T, Hamlington B (2021) Data-driven reconstruction reveals large-scale ocean circulation control on coastal sea level. *Nat Clim Change*. <https://doi.org/10.1038/s41558-021-01046-1>

- Deser C, Alexander M, Timlin M (1999) Evidence for a wind-driven intensification of the Kuroshio Current Extension from the 1970s to the 1980s. *J Clim* 12(6):1697–1706. [https://doi.org/10.1175/1520-0442\(1999\)012%3c1697:EFWDI%3e2.0.CO;2](https://doi.org/10.1175/1520-0442(1999)012%3c1697:EFWDI%3e2.0.CO;2)
- Dong C, McWilliams J, Liu Y, Chen D (2014) Global heat and salt transports by eddy movement. *Nat Commun* 5:3294. <https://doi.org/10.1038/ncomms4294>
- Ezer T (2015) Detecting changes in the transport of the Gulf Stream and the Atlantic overturning circulation from coastal sea level data: the extreme decline in 2009–2010 and estimated variations for 1935–2012. *Glob Planet Change* 129:23–36. <https://doi.org/10.1016/j.gloplacha.2015.03.002>
- Ezer T, Corlett WB (2012) Is sea level rise accelerating in the Chesapeake Bay? A demonstration of a novel new approach for analyzing sea level data. *Geophys Res Lett* 39(19):L19605. <https://doi.org/10.1029/2012GL053435>
- Ezer T, Dangendorf S (2020) Global sea level reconstruction for 1900–2015 reveals regional variability in ocean dynamics and an unprecedented long weakening in the Gulf Stream flow since the 1990s. *Ocean Sci* 16(4):997–1016. <https://doi.org/10.5194/os-2020-22>
- Ezer T, Dangendorf S (2021) Variability and upward trend in the kinetic energy of Western Boundary Currents over the last century: impacts from barostatic and dynamic sea level change. *Clim Dyn*. <https://doi.org/10.1007/s00382-021-05808-7>
- Ezer T, Atkinson LP, Corlett WB, Blanco JL (2013) Gulf Stream's induced sea level rise and variability along the U.S. mid-Atlantic coast. *J Geophys Res* 118:685–697. <https://doi.org/10.1002/jgrc.20091>
- Ezer T, Haigh ID, Woodworth PL (2016) Nonlinear sea-level trends and long-term variability on western European coasts. *J Coast Res* 32(4):744–755. <https://doi.org/10.2112/JCOAS-TRES-D-15-00165.1>
- Frederikse T, Landerer F, Caron L, Adhikari S, Parkes D, Humphrey VW, Dangendorf S, Hogarth P, Zanna L, Cheng L, Wu Y-H (2020) The causes of sea-level rise since 1900. *Nature* 584:393–397. <https://doi.org/10.1038/s41586-020-2591-3>
- Galperin B, Sukoriansky S, Qiu B (2021) Seasonal oceanic variability on meso- and submesoscales: turbulence perspective. *Ocean Dyn* 71. <https://doi.org/10.1007/s10236-021-01444-1>
- Gehrels WR, Dangendorf S, Barlow NLM, Saher MH, Long AJ, Woodworth PL, Piecuch CG, Berk K (2020) A preindustrial sea-level rise hotspot along the Atlantic coast of North America. *Geophys Res Lett* 47. <https://doi.org/10.1029/2019GL085814>
- Goddard PB, Yin J, Griffies SM, Zhang S (2015) An extreme event of sea-level rise along the Northeast coast of North America in 2009–2010. *Nat Commun*. <https://doi.org/10.1038/ncomms7346>
- Gregory JM, Griffies SM, Hughes CW, Lowe JA, Church JA, Fukimori I, Gomez N, Kopp RE, Landerer F, Le Cozannet G, Ponte RM, Stammer D, Tamisiea ME, van de Wal RSW (2019) Concepts and terminology for sea level: mean, variability and change, both local and global. *Surv Geophys* 40:1251–1289. <https://doi.org/10.1007/s10712-019-09525-z>
- Grinsted A, Moore JC, Jevrejeva S (2004) Application of the cross wavelet transform and wavelet coherence to geophysical time series. *Nonlin Processes Geophys* 11:561–566. <https://doi.org/10.5194/npg-11-561-2004>
- Han W, Stammer D, Thompson P, Ezer T, Palanisamy H, Zhang X, Domingues C, Zhang L, Yuan D (2019) Impact of basin-scale climate modes on coastal sea level: a review. *Surv Geophys* 40(6):1493–1541. <https://doi.org/10.1007/s10712-019-09562-8>
- Hay CH, Morrow E, Kopp RE, Mitrovica JX (2015) On the robustness of Bayesian fingerprinting estimates of global sea level change. *J Clim* 30:3025–3038. <https://doi.org/10.1175/JCLI-D-16-0271.1>
- Hu S, Sprintall J, Guan C, McPhaden MJ, Wang F, Hu D, Cai W (2020) Deep-reaching acceleration of global mean ocean circulation over the past two decades. *Sci Adv* 6(6). doi:<https://doi.org/10.1126/sciadv.aax7727>
- Hurrell JW (1995) Decadal trends in the North Atlantic Oscillation: regional temperatures and precipitation. *Science* 269:676–679
- Hurrell JW, Kushnir Y, Ottersen G, Visbeck M (eds) (2003) *The North Atlantic Oscillation: climate significance and environmental impact*. Geophys. Monogr. Ser, vol. 134. AGU, Washington, D. C
- Huang NE, Shen Z, Long SR, Wu MC, Shih EH, Zheng Q, Tung CC, Liu HH (1998) The empirical mode decomposition and the Hilbert spectrum for non stationary time series analysis. *Proc R Soc London Ser A* 45:903–995. <https://doi.org/10.1098/rspa.1998.0193>
- Jevrejeva S, Moore JC, Grinsted A, Woodworth PL (2008) Recent global sea level acceleration started over 200 years ago? *Geophys Res Lett* 35:L08715. <https://doi.org/10.1029/2008GL033611>
- Joyce TM, Deser C, Spall MA (2000) The relation between decadal variability of subtropical mode water and the North Atlantic oscillation. *J Clim* 13:2550–2569. [https://doi.org/10.1175/1520-0442\(2000\)013](https://doi.org/10.1175/1520-0442(2000)013)
- Kenigson JS, Han W, Rajagopalan B, Yanto JM (2018) Decadal shift of NAO-linked interannual sea level variability along the U.S. northeast coast. *J Clim* 31:4981–4989. <https://doi.org/10.1175/JCLI-D-17-0403.1>
- Little CM, Hu A, Hughes CW, McCarthy GD, Piecuch CG, Ponte RM, Thomas MD (2019) The relationship between U.S. East Coast sea level and the Atlantic Meridional Overturning Circulation: A review. *J Geophys Res* 124:6435–6458. <https://doi.org/10.1029/2019JC015152>
- Liu Y, Dong C, Guan Y, Chen D, McWilliams J, Nencioli F (2012) Eddy analysis in the subtropical zonal band of the North Pacific Ocean. *Deep Sea Res* 68:54–67. <https://doi.org/10.1016/j.dsr.2012.06.001>
- Mann ME, Park J (1996) Joint spatiotemporal modes of surface temperature and sea level pressure variability in the Northern Hemisphere during the last century. *J Clim* 9(9):2137–2162. [https://doi.org/10.1175/1520-0442\(1996\)009%3c2137:JSMOST%3e2.0.CO;2](https://doi.org/10.1175/1520-0442(1996)009%3c2137:JSMOST%3e2.0.CO;2)
- Martínez-Moreno J, Hogg AM, England MH, Constantinou NC, Kiss AE, Morrison AK (2021) Global changes in oceanic mesoscale currents over the satellite altimetry record. *Nat Clim Change* 11:397–403. <https://doi.org/10.1038/s41558-021-01006-9>
- McCarthy G, Frejka-Williams E, Johns WE, Baringer MO, Meinen CS, Bryden HL, Rayner D, Duchez A, Roberts C, Cunningham SA (2012) Observed interannual variability of the Atlantic meridional overturning circulation at 26.5°N. *Geophys Res Lett* 39(19). doi:<https://doi.org/10.1029/2012GL052933>
- Meinen CS, Baringer MO, Garcia RF (2010) Florida Current transport variability: an analysis of annual and longer-period signals. *Deep-Sea Res* 57(7):835–846. <https://doi.org/10.1016/j.dsr.2010.04.001>
- Merrifield MA, Merrifield ST, Mitchum GT (2009) An anomalous recent acceleration of global sea level rise. *J Clim* 22:5772–5781. <https://doi.org/10.1175/2009JCLI2985.1>
- Oey L-Y, Ezer T, Sturges W (2004) Modeled and observed Empirical Orthogonal Functions of currents in the Yucatan Channel. *J Geophys Res* 109:C08011. <https://doi.org/10.1029/2004JC002345>
- Rahmstorf S, Box J, Feulner G, Mann ME, Robinson A, Rutherford S, Schaffernicht EJ (2015) Exceptional twentieth-century slowdown in Atlantic Ocean overturning circulation. *Nature Clim Chan* 5:475–480. <https://doi.org/10.1038/nclimate2554>
- Sallenger AH, Doran KS, Howd P (2012) Hotspot of accelerated sea-level rise on the Atlantic coast of North America. *Nature Clim Chan* 2:884–888. <https://doi.org/10.1038/NCILMATE1597>
- Serazin G, Penduff T, Grégorio S, Barnier B, Molines J-M, Terray L (2015) Intrinsic variability of sea level from global 1/12° ocean simulations: spatiotemporal scales. *J Clim* 28(10):4279–4292. <https://doi.org/10.1175/JCLI-D-14-00554.1>

- Sen Gupta A, Stellema A, Pontes GM, Taschetto AS, Verges A, Rossi V (2021) Future changes to the upper ocean Western Boundary Currents across two generations of climate models. *Sci Rep* 11:9538. <https://doi.org/10.1038/s41598-021-88934-w>
- Smeed DA, Josey SA, Beaulieu C, Johns WE, Moat BI, Frajka-Williams E, Rayner D, Meinen CS, Baringer MO, Bryden HL, McCarthy GD (2018) The North Atlantic Ocean is in a State of reduced overturning. *Geophys Res. Lett.*, 45(3). doi:<https://doi.org/10.1002/2017GL076350>
- Taylor AH, Stephens JA (1998) The North Atlantic Oscillation and the latitude of the Gulf Stream. *Tellus A* 50(1):134–142. <https://doi.org/10.3402/tellusa.v50i1.14517>
- Tsimplis MN, Calafat FM, Marcos M, Jordá G, Gomis D, Fenoglio-Marc L, Struglia MV, Josey SA, Chambers DP (2013) The effect of the NAO on sea-level and on mass changes in the Mediterranean Sea. *J Geophys Res* 118:944–952. <https://doi.org/10.1002/jgrc.20078>
- Wu Z, Huang NE, Long SR, Peng C-K (2007) On the trend, detrending and variability of nonlinear and non-stationary time series. *Proc Nat Acad Sci* 104:14889–14894. <https://doi.org/10.1073/pnas.0701020104>
- Wu Z, Huang NE (2004) A study of the characteristics of white noise using the empirical mode decomposition method. *Proc Royal Soc* 460(2046). doi:<https://doi.org/10.1098/rspa.2003.1221>
- Wu Z, Huang NE (2009) Ensemble empirical mode decomposition: a noise-assisted data analysis method. *Adv Adapt Data Anal* 1(1):1–41. <https://doi.org/10.1142/S1793536909000047>
- Wu L, Cai W, Zhang L, Nakamura H, Timmermann A, Joyce T, McPhaden MJ, Alexander M, Qiu B, Visbeck M, Chang P, Giese B (2012) Enhanced warming over the global subtropical western boundary currents. *Nat Clim Chan* 2:161–166. <https://doi.org/10.1038/nclimate1353>
- Yang H, Lohmann G, Wei W, Dima M, Ionita M, Liu J (2016) Intensification and poleward shift of subtropical western boundary currents in a warming climate. *J Geophys Res* 121:4928–4945. <https://doi.org/10.1002/2015JC011513>
- Zhang W, Chai F, Xue H, Oey L-Y (2020) Remote sensing linear trends of the Gulf Stream from 1993 to 2016. *Ocean Dyn* 70:701–712. <https://doi.org/10.1007/s10236-020-01356-6>

Publisher's note Springer Nature remains neutral with regard to jurisdictional claims in published maps and institutional affiliations.